Detection of Antecedent Myocardial Ischemia With Multiselectin Molecular Imaging

Brian P. Davidson, MD, **Beat A. Kaufmann, MD**, **J. Todd Belcik, BS, RCS, RDCS**, **Aris Xie, MS**, **Yue Qi, MD**, and **Jonathan R. Lindner, MD**
Division of Cardiovascular Medicine, Oregon Health & Science University, Portland, Oregon

Abstract

Objective—Our aim was to develop an echocardiographic molecular imaging approach for detecting recent myocardial ischemia by using recombinant P-selectin glycoprotein ligand (PSGL)-1 as a targeting ligand, which is a feasible approach for human use.

Background—Ischemic memory imaging using human PSGL-1 as a targeting moiety may extend the time window for postischemic detection by targeting the early (P-selectin) and late (E-selectin) endothelial ischemic response.

Methods—Lipid microbubbles bearing recombinant human PSGL-1 (MB_{YSPSL}) or P-selectin antibody (MB_{Ab}) were prepared. Targeted attachment was evaluated by using flow chamber and intravital microscopy. In vivo ultrasound molecular imaging was first performed in the hindlimb in wild-type and P-selectin–deficient ($P^{-/-}$) mice 45 to 360 min after brief ischemia-reperfusion injury. Myocardial contrast echocardiography molecular imaging was performed 1.5, 3, 6, and 18 h after brief left anterior descending coronary artery ischemia-reperfusion.

Results—Microbubble attachment to P-selectin–immunoglobulin G fusion protein in flow chamber experiments (shear stress 0.5 to 8.0 dyne/cm^2) and to activated venular endothelium on intravital microscopy were similar for MB_{Ab} and MB_{YSPSL}. Intense enhancement was seen for MB_{Ab} and MB_{YSPSL} in postischemic muscle and was more stable over time for MB_{YSPSL}. On myocardial contrast echocardiography, both MB_{YSPSL} and MB_{Ab} produced similar signal enhancement at 90 min and 3 h after ischemia, which spatially correlated with the postischemic risk area. Signal significantly decreased but was still present at 6 to 18 h.

Conclusions—Echocardiographic molecular imaging with a human multi-selectin–targeted contrast agent bearing recombinant human PSGL-1 can detect myocardial ischemia hours after resolution. This approach may potentially be used for rapid bedside evaluation of patients with recent chest pain.

Keywords

contrast echocardiography; microbubbles; molecular imaging; myocardial ischemia; selectin

There are well-recognized limitations in the algorithms currently used to diagnose acute coronary syndromes (ACS) in patients who present with symptoms but whose initial electrocardiogram does not show ST-segment elevation (1–3). Various noninvasive imaging techniques have been proposed for improving diagnostic accuracy in patients with possible ACS. Molecular imaging has been used to detect biochemical alterations that occur not only

during ischemia but also persist after ischemia resolves. This approach, often referred to as ischemic memory imaging, may be particularly useful for detecting ischemia when the amount of necrosis is small or in patients who present after symptoms resolve or have pre-existing electrocardiogram or wall motion abnormalities. Ideally, molecular imaging should be able to detect and assess the spatial extent of ischemia hours after its resolution and provide information rapidly to the clinician.

Because of its portability and speed, myocardial contrast echocardiography (MCE) molecular imaging has been proposed as a point-of-care technique for rapidly detecting recent myocardial ischemia. MCE detection of myocardial ischemia after transient reduction in coronary flow has been achieved by targeting microbubble contrast agents to endothelial P-selectin (4,5). Selectins are a family of endothelial adhesion molecules that bind carbohydrate-bearing counter-ligands on leukocytes and are expressed in response to ischemia and other inflammatory stimuli (6,7). P-selectin is stored preformed in endothelial cells and expressed within minutes of ischemia or injury (8,9). However, the duration over which P-selectin imaging would be effective for detecting recent ischemia is uncertain because its surface expression tends to diminish over time after an ischemic insult. In the present study, we hypothesized that the time window for ischemic memory imaging could be extended by targeting not only P-selectin but also E-selectin, which exhibits delayed but more persistent expression for up to 24 h after endothelial activation (10–12). Accordingly, we developed a novel ultrasound contrast agent bearing a recombinant form of human P-selectin glyocoprotein (PSGL)-1, an endogenous counterligand for both P- and E-selectin. The use of recombinant human PSGL-1 as a targeting moiety also represents an important step toward the development of a human-ready agent for myocardial ischemic memory imaging with echocardiography.

Methods

Targeted microbubble preparation

Biotinylated lipid-shelled decafluorobutane microbubbles were prepared by sonication of an aqueous suspension of distearoylphosphatidylcholine, polyoxyethylene-40-stearate, and distearoyl-phosphatidylethanolamine-polyethylene glycol (PEG)(2000)-biotin in a 50:10:1 molar ratio. Conjugation of biotinylated ligand to the microbubble surface was performed by using a streptavidin bridge as previously described (13) to create the following agents: MB_{YSPSL}: bearing an immunoglobulin G (IgG) fusion protein with a dimeric recombinant form of the glycoprotein PSGL-1 (YSPSL, Y's Therapeutics Co., Ltd. Tokyo, Japan); MB_{Ab}: bearing rat anti-mouse P-selectin monoclonal antibody (mAb) (RB40.34, BD Pharmingen San Jose, California); or MB_{Ctr}: bearing iso-type control mAb (R3-34, BD Pharmingen). For flow chamber studies and intravital microscopy, MB_{Ab} and MB_{YSPSL} were fluorescently labeled by the addition of dioctadecyltetramethylindocarbocyanine or dioctadecyloxacarbocyanine perchlorate, respectively, to the microbubble shell. Perfusion imaging was performed with microbubbles lacking distearoyl-phosphatidylethanolamine-PEG(2000)-biotin. Microbubbles were analyzed for concentration and size distribution (Multisizer III, Beckman-Coulter, Brea, California). Intravascular half-life for each agent was determined by left ventricular cavity intensity on MCE after intravenous injection of 5×10^6 microbubbles.

Flow chamber attachment

Cell culture dishes were coated with an IgG fusion protein bearing murine P-selectin (BD Pharmingen Inc.) at a site density of approximately 100 μm^{-1}(14). The dishes were blocked with 3% bovine serum albumin and mounted on a parallel plate flow chamber (Glycotech Inc. Gaithersburg, Maryland) that was placed in an inverted position on a microscope

(Axioskop2-FS, Carl Zeiss Inc. Thornwood, New York) for video recording. Suspensions of fluorescently labeled MB_{YSPSL} and MB_{Ab} (3×10^6 ml^{-1}) were drawn through the flow chamber at flow rates resulting in calculated shear stresses of 0.5, 1.0, 2.0, or 8.0 dynes/cm^2. The number of microbubbles attached to the plate was determined for 20 optical fields after 3 min of continuous flow. Experiments were performed in duplicate for each condition.

Animal preparation

Studies were approved by the Animal Care and Use Committee at Oregon Health & Science University. Male wild-type C57Bl/6 mice and P-selectin– deficient (P$^{-/-}$) mice (Jackson Labs) 10 to 15 weeks of age were studied. For intravital microscopy, mice were anesthetized with an intraperitoneal injection (12.5 μl/g) of a solution containing ketamine hydrochloride (10 mg/ml), xylazine (1 mg/ml), and atropine (0.02 mg/ml). For molecular imaging, mice were anesthetized with inhaled iso-flurane (0.75% to 1.5% for maintenance). A jugular vein was cannulated for injection of microbubbles.

Intravital microscopy

A cremaster muscle in wild-type mice (n = 3) was prepared as previously described (15). Video recordings were made with a microscope and recorded with a charge-coupled device camera (C2400, Hamamatsu Photonics). Muscle preparations were studied 20 to 30 min after exteriorization, and P-selectin expression from surgical trauma was confirmed by the presence of leukocyte rolling in postcapillary venules (9). Fluorescently labeled MB_{YSPSL} and MB_{Ab} (1×10^7) were simultaneously injected intravenously. Microbubble attachment in 10 to 15 randomly selected optical fields was quantified 2 to 4 min after injection using fluorescent epi-illumination.

Contrast-enhanced ultrasound

Imaging was performed with a linear array transducer (15L8) interfaced with a Sequoia ultrasound system (Siemens Medical Systems, Mountain View, California). A multipulse algorithm using phase and amplitude modulation was used to detect the nonlinear fundamental component of the microbubble signal. Imaging was performed at a centerline frequency of 7 MHz.

Hindlimb molecular imaging protocol

Contrast-enhanced ultrasound molecular imaging of the proximal hindlimb adductor muscles was performed after unilateral ischemia-reperfusion injury produced by tourniquet occlusion for 10 min. Ischemia was confirmed by a >95% reduction in flow according to contrast-enhanced ultrasound perfusion imaging. Molecular imaging was performed in the postischemic limb at 45, 90, 180, and 360 min after ischemia in 20 wild-type and 9 P$^{-/-}$ mice and bilaterally in 3 control wild-type mice not undergoing ischemia-reperfusion. In 4 additional P$^{-/-}$ mice, imaging was performed at 360 min after blocking E-selectin by intravenous injection of rat anti-mouse E-selectin mAb (UZ4, Millipore Billerica, Massachusetts). Imaging was performed by using low power imaging (mechanical index [MI] 0.18) 8 min after intravenous injection of MB_{YSPSL} and MB_{Ab} (1×10^7) performed in random order. Comparison of control microbubble (MB_{Ctr}) to both targeted agents was performed in an additional 12 wild-type and 6 P$^{-/-}$ mice at the 45 min postischemic time interval only. For all image sets, signal for retained microbubbles alone was derived by digitally subtracting the signal from freely circulating microbubbles as previously described (13).

Myocardial molecular imaging protocol

Mice were placed on positive-pressure ventilation. Ligature occlusion of the LAD through a left lateral thoracotomy was performed to produce brief myocardial ischemia confirmed by ST-segment elevation on electrocardiogram monitoring. The ligature was released after 10 min but was left in place, and the chest wall was closed. Mice were extubated, and wall motion was assessed within 10 min of reperfusion and again at 3 h using high-frequency (30 MHz) echocardiography (Vevo 770, Visualsonics, Toronto, Ontario, Canada) in the midventricular short-axis plane. MCE molecular imaging was performed in the same imaging plane at 1.5 and 3 h in 8 wild-type mice or at 6 and 18 h in 6 wild-type mice. In 2 $P^{-/-}$ mice, imaging was performed at the intermediate postischemic intervals (3 and 6 h). Imaging was performed 3 and 6 h after sham surgery with ligature placement but no occlusion in 3 wild-type mice. For molecular imaging, first low MI (0.16) then high MI (1.4) imaging was performed 8 min after injection of 5×10^6 MB_{Ab} or MB_{YSPSL} in random order. Several end-systolic images were acquired and averaged, and signal for retained microbubbles alone was derived by digitally subtracting the signal from freely circulating microbubbles at the appropriate MI (Online Fig. 1) (13). After completion of molecular imaging, the ischemic risk area was measured by reopening the chest, retying the LAD ligature, and injecting 1×10^{11} fluorescently labeled 500 nm polystyrene nanospheres (Duke Scientific Corp. Palo Alto, California) intravenously. After 2 min of circulation time, the heart was removed, and a 1-mm short-axis section corresponding to the echocardiographic imaging plane was examined by using fluorescent microscopy. The fluorescent-free risk area was used to guide region-of-interest selection for MCE molecular imaging and quantitative wall motion analysis. The risk area averaged from the basal and apical aspects of the histological slice and the area of enhancement on molecular imaging were measured independently by readers blinded to animal identity. In selected animals, the left ventricle was divided in 1-mm short-axis slices and stained with 2,3,5-triphenyltetrazolium chloride to exclude infarction.

Statistical analysis

Comparisons between microbubble agents for the flow chamber studies and intravital microscopy were made with a Mann-Whitney rank-sum test. For both, paired analysis was performed on a per-optical field basis. For multiple comparisons of the in vivo imaging data, a Kruskal-Wallis test with Dunn's post-hoc test was used. Differences were considered significant at $p < 0.05$.

Results

Microbubble attachment in physiological shear

Microbubble size distribution was similar between targeted microbubble agents, and intravascular half-life was slightly shorter for MB_{Ab} compared with MB_{YSPSL} (Online Figs. 2 and 3). Flow chamber experiments demonstrated that firm adhesion of microbubbles to P-selectin–IgG fusion protein was similar for MB_{YSPSL} and MB_{Ab} across a range of shear stresses (Fig. 1).

Surgical exteriorization of the cremaster muscle for intra-vital microscopy produced leukocyte rolling (10 to 110 μm/s) in postcapillary venules consistent with endothelial selectin expression (9). Endothelial attachment of microbubbles after intravenous injection was similar for MB_{YSPSL} and MB_{Ab} (Fig. 2, Online Videos 1, 2, and 3) and occurred almost exclusively in post-capillary venules. Microbubble rolling along the venular endothelial surface was occasionally observed only with MB_{YSPSL}, which constituted <10% of all endothelial-microbubble interactions. Leukocyte rolling was observed in all venular segments in which microbubble attachment was seen.

Molecular imaging in postischemic skeletal muscle

As an initial step to evaluate temporal patterns of microbubble retention, hindlimb ischemia was used because of the stability of the preparation. Strong signal enhancement 45 min after ischemia from both targeted agents was detected in wild-type mice, which was not seen in postischemic $P^{-/-}$ mice, in nonischemic controls, or from control microbubbles in any treatment group (Fig. 3). Temporal characterization was therefore performed only for targeted agents (Fig. 4). Signal from MB_{Ab} in the postischemic limb of wild-type mice peaked at 90 min after reflow and then diminished over time so that signal intensity had decreased by approximately one-half at 6 h (Fig. 4A). Lower signal was found at all time points for MB_{YSPSL}, yet the signal produced by this agent remained more stable over time. In $P^{-/-}$ mice, there was no signal enhancement in the ischemic limb for MB_{Ab} at all time points, whereas MB_{YSPSL} produced late signal enhancement that, at 6 h, was similar in intensity to that in wild-type mice (Fig. 4B) and was abolished by blocking E-selectin.

Post-ischemic imaging of the myocardium

For mice undergoing transient LAD ischemia, the mean risk area was 46% of the myocardial area (range 24% to 61%). Shortly after reperfusion, a reduction in radial wall thickening fraction was seen in the center of the risk area compared with the remote region (0.12 ± 0.10 vs 0.33 ± 0.08, $p < 0.01$), which resolved when remeasured at 3 h (0.25 ± 0.08 vs 0.28 ± 0.07), consistent with brief postischemic stunning. Postmortem 2,3,5-triphenyltetrazolium chloride staining did not detect myocardial infarction in any slice (Online Fig. 4). At 1.5 and 3 h after ischemic injury, MB_{YSPSL} and MB_{Ab} produced strong and equivalent signal enhancement in the postischemic territory for both low- and high-power imaging (Figs. 5A and 5C; log-linear transformed data in Online Fig. 5). At 6 and 18 h, targeted signal was much lower and not significantly different from the remote nonischemic regions. Very low signal enhancement was seen in control experiments (Figs. 5B and 5D), which included nonsurgical controls, sham-operated animals, and $P^{-/-}$ mice undergoing ischemic injury. Data from sham-operated experiments indicated that signal from targeted agents in the remote nonischemic zone was likely an artifact of injury from the open-chest preparation. The spatial territory of enhancement from MB_{YSPSL} and MB_{Ab} correlated modestly with the spatial extent of the risk area (Fig. 6). The correlation was better at 1.5 than 3 h due primarily to a time-dependent reduction in the area of ultrasound enhancement.

Discussion

In this study, we developed and evaluated a novel approach to echocardiographic ischemic memory imaging by using a multi-selectin–targeted microbubble contrast agent bearing human recombinant dimeric PSGL-1. This agent not only represents a feasible approach for human imaging but also has the potential to extend the time window for detecting recent ischemia by targeting E-selectin. In murine models of ischemia, this dual-selectin–targeted agent was able to detect and spatially represent recent ischemia without infarction. It had a more stable quantitative signal over time than mAb-based targeting in skeletal muscle but not the heart.

Interest in ischemic memory imaging is a consequence of the diagnostic challenges in patients who present with acute chest pain or other possible ischemic symptoms. In patients who have ACS, the electrocardiogram and serological markers are often nondiagnostic, leading to delayed or even missed diagnosis. Furthermore, there are disease states other than ischemia that can result in false-positive or uninterpretable results for these tests. Methods to noninvasively image myocardial ischemia are being developed in response to these recognized limitations. Moreover, in those patients who have recognized ACS, defining the

spatial extent of ischemia can be potentially useful for stratifying treatment according to the amount of myocardium at risk.

Interest in an echocardiographic approach is based on practical issues such as cost, availability, and speed. Echocardiographic imaging of wall motion and perfusion in the emergency department can provide rapid diagnostic and prognostic information in patients who have chest pain (16). This information may be of limited value when performed late after resolution of symptoms or in those with pre-existing abnormalities in perfusion and/or function. Molecular imaging of ischemia for diagnosis of ACS is contingent on the ability to detect events that occur rapidly at the onset of ischemia and persist for hours after resolution. For imaging recent ischemia, microbubbles have been targeted to P-selectin via the conjugation of either mAb or selectin-specific carbohydrates to their surface (4,5,13). Although initial reports of using P-selectin to detect injury were made using renal ischemia, recent studies have confirmed that it is also possible to detect myocardial ischemia without infarction.

In this study, the use of human recombinant dimeric PSGL-1 as a targeting moiety represents an important step toward a human-ready agent. This molecule has the necessary carbohydrate modifications required for selectin binding and has been investigated as an immunomodulatory agent in human clinical trials (17). The ability to target multiple selectins is potentially an advantage because postischemic selectin expression has an early phase involving preformed P-selectin stored within the Weibal-Palade bodies of endothelial cells and a later phase expression that includes E-selectin. Thus, we hypothesized that the ability to target both selectins would extend the time window for which it is possible to detect recent ischemia.

The in vitro and in vivo adhesion studies indicated a similar degree of attachment at various shear rates for mAb- and PSGL-1–targeting approaches. On intravital microscopy, surgical preparation of the cremaster muscle typically produces heterogeneity in the amount of venular leukocyte rolling. Microbubble attachment occurred only in venular segments with rolling leukocytes. Microbubble attachment to immobilized platelets, which also express P-selectin particularly on activation, was not observed, although we did not use a model that produces much platelet adhesion. Rolling before adhesion was not a frequent finding on intravital microscopy.

Mouse hindlimb imaging was used as a reproducible model for characterizing the temporal course of microbubble retention after ischemia. These experiments indicated that MB_{YSPSL} had a more stable degree of postischemic enhancement than MB_{Ab}. This attribute, according to $P^{-/-}$ mouse data, was attributable to the MB_{YSPSL} binding to delayed E-selectin expression.

For myocardial ischemic memory imaging, our data suggest that selectin targeting provides robust information on the presence of ischemia for several hours after resolution. The mAb and PSGL-1 approaches provided relatively equivalent signal. Signal enhancement even at 6 h was largely suppressed in $P^{-/-}$ mice. These data suggest less of a contribution of E-selectin to MB_{YSPSL} signal in the myocardium compared with skeletal muscle. However, because rolling or adhesion of leukocytes and, by inference, microbubbles is dependent on the interacting types and numbers of ligand-counterligand bonds, the $P^{-/-}$ data do not necessarily exclude the contribution of E-selectin to late postischemic myocardial signal enhancement. Our data also suggest that molecular imaging can provide a relatively accurate representation of the spatial extent of recent ischemia only if performed relatively early (3 h) after injury, although results in humans may certainly differ. The correlations between risk area and enhancement area were only modest. We believe this finding is primarily due

to several factors, the first being related to scale in which there is difficulty coregistering MCE molecular imaging data, which were averaged from a 1.0- to 1.2-mm beam elevation (thickness) with a single slice obtained for nanosphere-derived risk area, a factor underscored by the finding on several histological slices that the nanosphere-derived risk area varied by as much as 8% of total area depending on whether the basal or apical aspect of the slice was examined. The second factor is the likelihood for selectin expression in ischemic regions extending beyond the area that lacked nanospheres because risk area was defined as the territory completely void of nanospheres.

The disparity in signal intensity and the degradation of signal over time for MB_{Ab} versus MB_{YSPSL} for the hindlimb and myocardial studies may be explained several ways. Although the ischemic duration was very brief for both models, the degree of ischemia was probably greater for the myocardium due to higher oxygen debt. Second, there are data to suggest that basal and inducible expression of endothelial adhesion molecules in the microcirculation can differ according to tissue type (10,18,19). The greater severity of ischemia in the myocardium may have produced a greater degree of E-selectin expression and a longer duration of signal enhancement for MB_{YSPSL} (20).

Study limitations

There are several limitations of this study that deserve attention. Endothelial surface expression of selectins was not quantified because there is no available method to do so. It is also possible that intravascular activation and recruitment of leukocytes may have contributed to postischemic tissue signal by nonspecific microbubble-leukocyte attachment, although previous studies indicate that the contribution of this is minimal (13). We did not vary the duration of ischemic insult and instead used only a very mild degree of ischemia to test our agents. For future use in humans, ligand conjugation strategies other than biotin-streptavidin are being used, and pharmacology and toxicology will need to be evaluated. We do not believe this change in formulation reduces the impact of this study because the use of a PEG spacer and stoichiometry of the ligand will probably not differ substantially for the human-ready agent. Finally, we used recombinant human PSGL-1 in murine models of ischemia. The relative benefit of using a dual selectin-targeted imaging agent and the duration that ischemia can be detected may be different in humans.

Conclusions

We found that a recombinant form of the endogenous ligand for P- and E-selectin as a targeting ligand could be used to detect recent myocardial ischemia for a several hours after its resolution even when wall motion had normalized. This imaging strategy offers a potentially useful rapid bedside risk stratification tool to not only detect recent myocardial ischemic but also to evaluate the spatial extent of myocardium at risk.

Supplementary Material

Refer to Web version on PubMed Central for supplementary material.

Acknowledgments

Abbreviations and Acronyms

ACS	acute coronary syndrome
IgG	immunoglobulin G
LAD	left anterior descending coronary artery
mAb	monoclonal antibody
MB$_{Ab}$	microbubbles bearing P-selectin antibody
MB$_{YSPSL}$	microbubbles bearing recombinant human P-selectin glycoprotein ligand-1
MCE	myocardial contrast echocardiography
MI	mechanical index
PEG	polyethylene glycol
PSGL	P-selectin glycoprotein ligand

References

1. Eagle KA, Goodman SG, Avezum Á, Budaj A, Sullivan CM, López-Sendón J. Practice variation and missed opportunities for reperfusion in ST-segment-elevation myocardial infarction: findings from the Global Registry of Acute Coronary Events (GRACE). Lancet. 2002; 359:373–7. [PubMed: 11844506]

2. Mehta RH, Eagle KA. Missed diagnoses of acute coronary syndromes in the emergency room—continuing challenges. N Engl J Med. 2000; 342:1207–10. [PubMed: 10770988]

3. Brieger D, Eagle KA, Goodman SG, et al. Acute coronary syndromes without chest pain, an underdiagnosed and undertreated high-risk group: insights from the global registry of acute coronary events. Chest. 2004; 126:461–9. [PubMed: 15302732]

4. Kaufmann BA, Lewis C, Xie A, Mirza-Mohd A, Lindner JR. Detection of recent myocardial ischaemia by molecular imaging of P-selectin with targeted contrast echocardiography. Eur Heart J. 2007; 28:2011–7. [PubMed: 17526905]

5. Villanueva FS, Lu E, Bowry S, et al. Myocardial ischemic memory imaging with molecular echocardiography. Circulation. 2007; 115:345–52. [PubMed: 17210843]

6. Bevilacqua MP, Nelson RM. Selectins. J Clin Invest. 1993; 91:379–87. [PubMed: 7679406]

7. Ley K. The role of selectins in inflammation and disease. Trend Mol Med. 2003; 9:263–8.

8. Chukwuemeka AO, Brown KA, Venn GE, Chambers DJ. Changes in P-selectin expression on cardiac microvessels in blood-perfused rat hearts subjected to ischemia-reperfusion. Ann Thorac Surg. 2005; 79:204–11. [PubMed: 15620944]

9. Ley K, Bullard DC, Arbones ML, et al. Sequential contribution of L- and P-selectin to leukocyte rolling in vivo. J Exp Med. 1995; 181:669–75. [PubMed: 7530761]

10. Haraldsen G, Kvale D, Lein B, Farstad IN, Brandtzaeg P. Cytokine-regulated expression of E-selectin, intercellular adhesion molecule-1 (ICAM-1), and vascular cell adhesion molecule-1 (VCAM-1) in human intestinal microvascular endothelial cells. J Immunol. 1996; 156:2558–65. [PubMed: 8786319]

11. Jones SP, Trocha SD, Strange MB, et al. Leukocyte and endothelial cell adhesion molecules in a chronic murine model of myocardial reperfusion injury. Am J Physiol Heart Circ Physiol. 2000; 279:H2196–201. [PubMed: 11045953]

12. Weyrich AS, Buerke M, Albertine KH, Lefer AM. Time course of coronary vascular endothelial adhesion molecule expression during reperfusion of the ischemic feline myocardium. J Leukoc Biol. 1995; 57:45–55. [PubMed: 7530283]

13. Lindner JR, Song J, Christiansen J, Klibanov AL, Xu F, Ley K. Ultrasound assessment of inflammation and renal tissue injury with microbubbles targeted to P-selectin. Circulation. 2001; 104:2107–12. [PubMed: 11673354]

14. Takalkar AM, Klibanov AL, Rychak JJ, Lindner JR, Ley K. Binding and detachment dynamics of microbubbles targeted to P-selectin under controlled shear flow. J Control Release. 2004; 96:473–82. [PubMed: 15120903]

15. Lindner J, Coggins M, Kaul S, Klibanov A, Brandenburger G, Ley K. Microbubble persistence in the microcirculation during ischemia/reperfusion and inflammation is caused by integrin and compliment mediated adherence to activated leukocytes. Circulation. 2000; 101:668–75. [PubMed: 10673260]

16. Wei K, Peters D, Belcik T, et al. A predictive instrument using contrast echocardiography in patients presenting to the emergency department with chest pain and without ST-segment elevation. J Am Soc Echocardiogr. 2010; 23:636–42. [PubMed: 20418056]

17. Gaber AO, Mulgaonkar S, Kahan BD, et al. YSPSL (rPSGL-Ig) for improvement of early renal allograft function: a double-blind, placebo-controlled multicenter Phase IIa study. Clin Transplant. 2010; 25:523–33. [PubMed: 20573162]

18. Hickey MJ, Kanwar S, McCafferty DM, Granger DN, Eppihimer MJ, Kubes P. Varying roles of E-electin and P-selectin in different microvascular beds in response to antigen. J Immunol. 1999; 162:1137–43. [PubMed: 9916744]

19. Yan J, Nunn AD, Thomas R. Selective induction of cell adhesion molecules by proinflammatory mediators in human cardiac microvascular endothelial cells in culture. Int J Clin Exp Med. 2010; 3:315–31. [PubMed: 21072266]

20. Russell J, Epstein CJ, Grisham MB, Alexander JS, Yeh KY, Granger DN. Regulation of E-selectin expression in postischemic intestinal microvasculature. Am J Physiol Gastrointest Liver Physiol. 2000; 278:G878–85. [PubMed: 10859217]

APPENDIX

For supplementary figures and videos, please see the online version of this article.
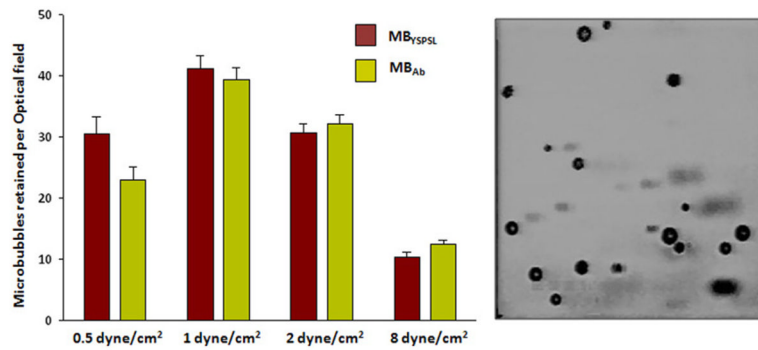
Figure 1. In Vitro Attachment of Targeted Microbubbles

Mean ± SEM number of targeted microbubbles attached to P-selectin–immunoglobulin G fusion protein (site density of $\approx 100 \ \mu m^{-1}$) in a flow chamber under various shear stresses. Each optical field represents 0.09 mm^2. Microbubble adhesion in the flow chamber is illustrated to the **right.** MB$_{Ab}$ = microbubbles bearing P-selectin antibody; MB$_{YSPSL}$ = microbubbles bearing recombinant human P-selectin glycoprotein ligand-1.
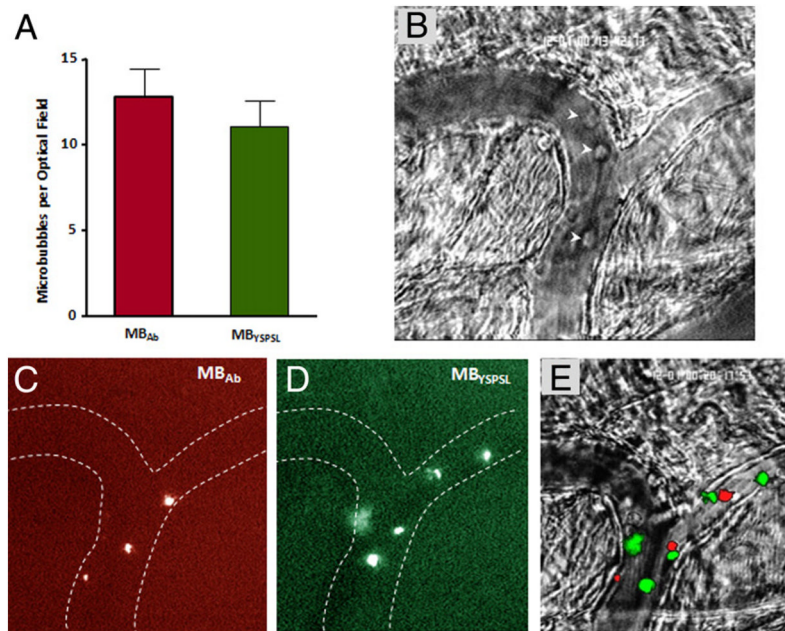
Figure 2. Microbubble Attachment to Mouse Cremasteric Venules
(A) Mean ± SEM number of retained microbubbles per optical field. Intravital microscopy images of the cremaster muscle illustrate **(B)** converging venules with rolling leukocytes **(arrowheads)** on bright field microscopy, **(C)** venular adhesion of dioctadecyltetramethylindocarbocyanine-labeled MB_{Ab}, **(D)** venular adhesion of dioctadecyloxacarbocyanine-labeled MB_{YSPSL}, and **(E)** merged images. Also see Online Videos Online Videos 1, 2, and 3. Abbreviations as in Figure 1.
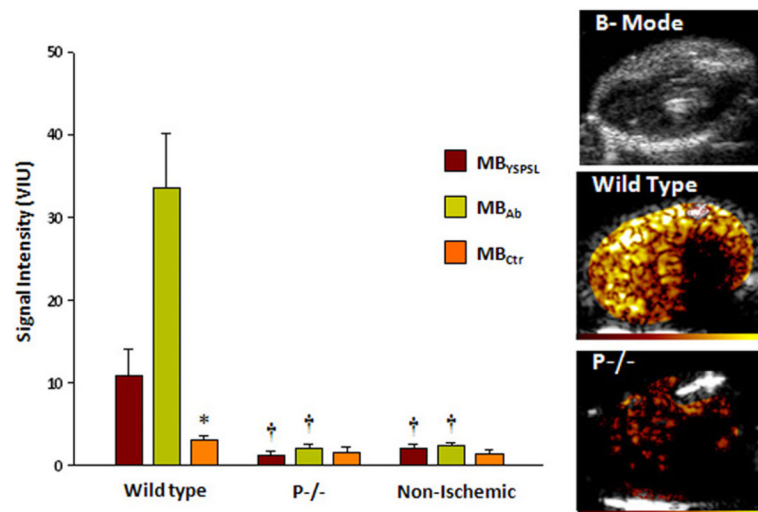
Figure 3. Molecular Imaging 45 min After Ischemia-Reperfusion Injury of the Hindlimb
Mean ± SEM video intensity for control microbubbles (MB_{Ctr}) and selectin-targeted microbubbles in the post-ischemic proximal hindlimb adductor muscles in wild-type and P-selectin–deficient ($P^{-/-}$) mice, and in control mice not undergoing ischemia. Examples illustrate hindlimb two-dimensional anatomy and contrast-enhanced ultra- sound molecular imaging with MB_{Ab} after ischemia in a wild-type and $P^{-/-}$ mice. Color scale at bottom. *p < 0.05 versus targeted agents; †p < 0.01 versus wild-type. Abbreviations as in Figure 1.
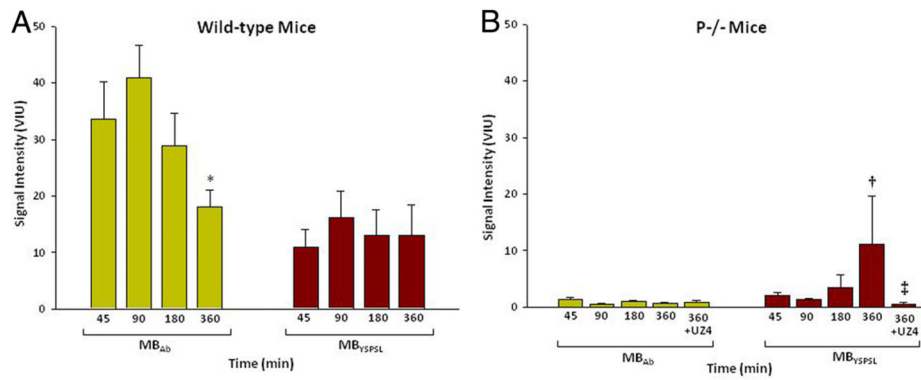
Figure 4. Molecular Imaging Signal in the Post-Ischemic Hindlimb at Various Reperfusion Intervals

Mean $\pm$ SEM video intensity for selectin-targeted microbubbles (MB_{Ab} and MB_{YSPSL}) in the proximal hindlimb adductor muscles of the postischemic limb in **(A)** wild-type and **(B)** P-selectin–deficient mice ($P^{-/-}$). UZ4 = anti–E-selectin monoclonal antibody; other abbreviations as in Figure 1. *p < 0.05 versus 90 min; †p < 0.05 versus 45 to 180 min; ‡p < 0.05 versus corresponding untreated data at 360 min.
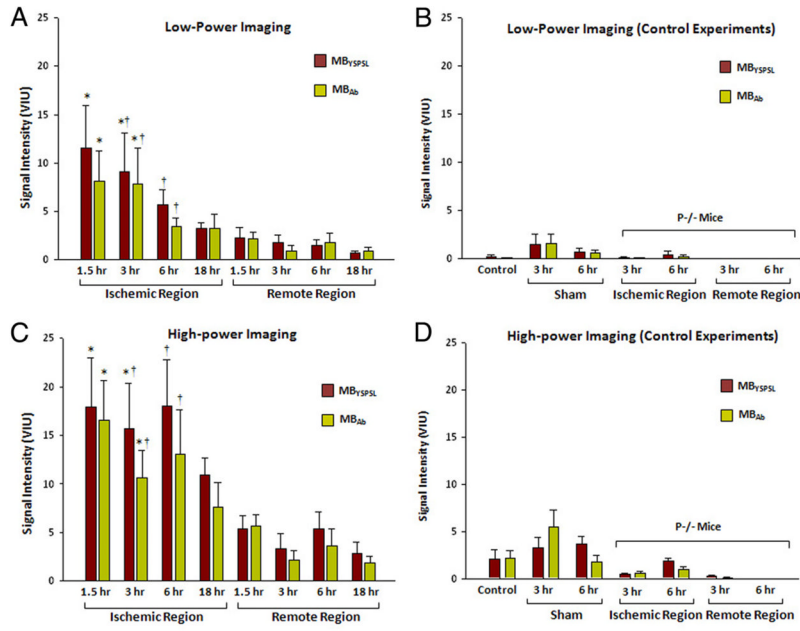
Figure 5. Signal Enhancement From Myocardial Ischemic Memory Imaging With Selectin-Targeted Microbubbles

Data represent mean ± SEM video intensity. **(A)** Low-power imaging data in wild-type mice undergoing ischemia-reperfusion injury of the left anterior descending coronary artery (LAD). **(B)** Low-power control experiments, which include nonsurgical control animals, sham-operated animals at 3 and 6 h, and P-selectin–deficient ($P^{-/-}$) mice undergoing LAD ischemia-reperfusion injury. **(C)** High-power imaging data in wild-type mice undergoing ischemia-reperfusion injury of the LAD. **(D)** High-power control experiments. *p < 0.05 versus remote territory; †p < 0.05 versus ischemic territory in $P^{-/-}$ mice. Abbreviations as in Figure 1.
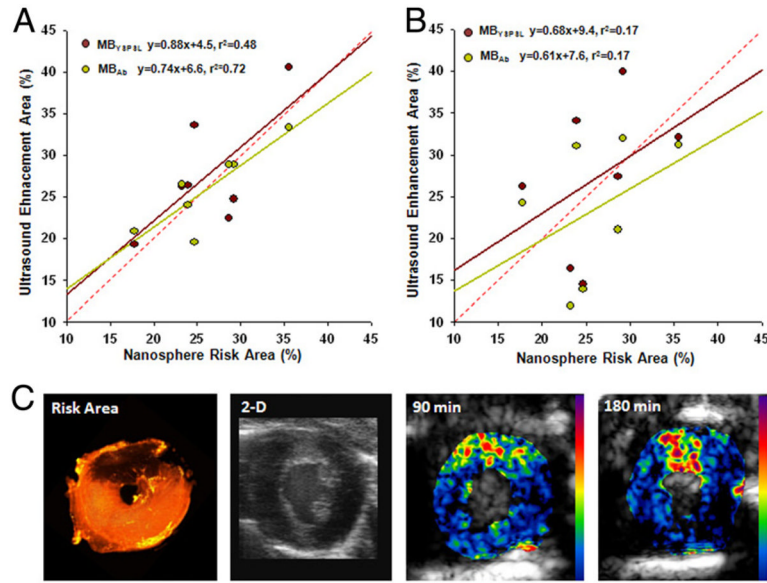
Figure 6. Spatial Assessment of Recent Ischemia With Molecular Imaging
Relation between risk area determined by fluorescent nanospheres and region of enhancement during molecular imaging at either **(A)** 90 min or **(B)** 3 h. Regression **line colors** correspond to their respective data points; **red dashed line** = line of identity; $p < 0.05$ only for 90-min correlations. **(C)** Example of a myocardial short-axis section illustrating the nanosphere-derived risk area in the anterior myocardium **(dark region)**, two-dimensional high-frequency imaging as an anatomic reference, and myocardial contrast echocardiography molecular imaging with MB_{YSPSL} obtained 90 min and 3 h after left anterior descending coronary artery ischemia-reperfusion injury. Cavity size differences are due to postmortem contracture. Abbreviations as in Figure 1.